Nonequilibrium dark space phase transition

Federico Carollo[1,*] and Igor Lesanovsky[1,2]

[1] *Institut für Theoretische Physik, Eberhard Karls Universität Tübingen, Auf der Morgenstelle 14, 72076 Tübingen, Germany*

[2] *School of Physics and Astronomy and Centre for the Mathematics and Theoretical Physics of Quantum Non-Equilibrium Systems, The University of Nottingham, Nottingham, NG7 2RD, United Kingdom*

We introduce the concept of dark space phase transition, which may occur in open many-body quantum systems where irreversible decay, interactions and quantum interference compete. Our study is based on a quantum many-body model, that is inspired by classical nonequilibrium processes which feature phase transitions into an absorbing state, such as epidemic spreading. The possibility for different dynamical paths to interfere quantum mechanically results in collective dynamical behavior without classical counterpart. We identify two competing dark states, a trivial one corresponding to a classical absorbing state and an emergent one which is quantum coherent. We establish a nonequilibrium phase transition within this dark space that features a phenomenology which cannot be encountered in classical systems. Such emergent two-dimensional dark space may find technological applications, e.g. for the collective encoding of a quantum information.

A dark (or absorbing) state is a non-fluctuating state that once it is reached during the course of a time-evolution it cannot be left. Dynamical systems that possess a dark state can display complex nonequilibrium behavior and universal dynamical scaling, even in low dimensions [1–3]. Remarkably, many real-world processes actually feature such dark state, as, for instance, the epidemic spreading of a virus among a population [4, 5]: for sufficiently low infection rate the population reaches a dark state, where all units are healthy and the virus is eradicated. However, when the infection rate is increased a stationary state phase transition to a fluctuating phase can take place. Here the virus becomes endemic and an extensive number of units remains infected. Interestingly, also dissipative quantum processes can feature dark states and allow to explore related concepts and phenomena in an entirely different setting. However, the phenomenology of systems studied so far [6–13] is closely related to that of classical processes.

In this paper, we report analytical and numerical evidence for the existence of a novel type of dark state phase transition, which has no classical counterpart as it crucially relies on quantum interference. To illustrate this new phenomenology we utilize a quantum many-body system, composed of N units which can be found in three different states [shown in Fig. 1(a)]. Using the analogy of epidemic spreading, one state represents a healthy unit, denoted as $|\circ\rangle$. The second state, $|*\rangle$, represents instead an infected but not contagious unit, while the third, $|\bullet\rangle$, represents an infected unit which is also contagious and can thus spread the virus. The dynamics of these units is subject to a classical process — the recovery process — consisting of transitions from state $|*\rangle$ to the $|\circ\rangle$, which competes with two other processes that are quantum coherent. The first one connects the contagious and not contagious states. The second one can be regarded as a quantum analogue of an infection process: coherent transitions between the state $|\circ\rangle$ and $|*\rangle$ take place, provided that at least one of the neighbors of the unit is in the contagious state [see Fig. 1(b)].

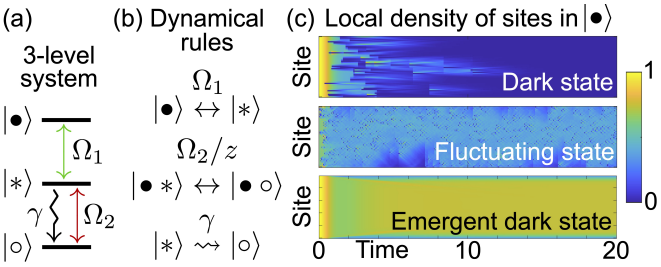

FIG. 1. **Dark state phase transition**. (a) Three-level quantum system with basis states $|\bullet\rangle$,$|*\rangle$ representing contagious and non contagious infected units, and the healthy state $|\circ\rangle$. (b) The dynamics consists of coherent transitions between infected states $|\bullet\rangle \leftrightarrow |*\rangle$ (rate Ω_1) and between states $|\circ\rangle \leftrightarrow |*\rangle$. This (infection) process must be facilitated by the presence of a contagious neighbor. For each contagious neighbor, the rate of the process is enhanced by a factor Ω_2/z, where z is the coordination number of the lattice. (c) Illustrative trajectories for a $1D$ quantum system with 50 sites. Top: Approach to the dark state $|\mathrm{D}\rangle$ for the model depicted in (a). Middle: Fluctuating phase which typically emerges in classical and quantum models with absorbing states. The example shown is for the quantum contact process [9]. Bottom: Emergence of the dark state $|\mathrm{D_e}\rangle$ for the model in depicted in (a).

According to these dynamical rules, the state with all healthy units, $|\mathrm{D}\rangle$, is an exact dark state for any system size N. Indeed, such state has no contagious unit that may activate the spreading of the infection [see Fig. 1(c)]. Typically, for both classical and quantum dark state phase transitions [1–3, 6–10, 12], one observes, for increasing infection rate, the emergence of a second steady state with finite density $\varrho_\bullet$ of contagious sites. This state exhibits dynamical fluctuations [cf. Fig. 1(c)]. However,

the model depicted in Fig. 1(a) displays behavior which is markedly different: the second stationary state is an emergent dark state $|\mathrm{D_e}\rangle$, which shows no fluctuations [cf. Fig. 1(c)] and — contrary to the state $|\mathrm{D}\rangle$ — it is a genuine quantum state characterized by units being in a superposition of contagious and healthy states. The emergence of this state is connected to destructive interference between coherent transition channels, similar to electromagnetically induced transparency [14]. Here, however, interference stems from interactions and is not a single-body effect. Beyond the novel phase transition phenomenology, the emergent dark manifold could potentially play a role in quantum information. The two dark states encode a qubit state $|\Psi\rangle = \alpha\,|\mathrm{D}\rangle + \beta\,|\mathrm{D_e}\rangle$ and the robustness of these two non-fluctuating stationary phases could provide an efficient self-correcting mechanism.

The model.— The elementary processes of the considered many-body quantum system are shown in Fig. 1(a). It consists of N three-level units, which are arranged in a D-dimensional lattice and follow a stochastic Markovian evolution [15] whose dynamical realizations (quantum trajectories) are governed by a random process through a stochastic Schrödinger equation [15, 16]. It is convenient to first introduce the deterministic time-evolution of the quantum state averaged over all trajectories. This state is described, at any time t, by the density operator ρ_t which obeys the quantum master equation [17, 18]

$$\frac{d}{dt}\rho_t = \mathcal{L}[\rho_t] = -i[H,\rho_t] + \mathcal{D}\left[\rho_t\right]. \tag{1}$$

The super-operator

$$\mathcal{D}[\rho] = \gamma \sum_{k=1}^{L}\left(J_-^{(k)}\rho J_+^{(k)} - \frac{1}{2}\left\{J_+^{(k)}J_-^{(k)},\rho\right\}\right) \tag{2}$$

is the so-called dissipator. In our case, it accounts for the classical (irreversible) transitions from the infected state $|*\rangle$ to the healthy one $|\circ\rangle$ [cf. Fig. 1(b)], and the jump operator $J_- = |\circ\rangle\langle *|$ (with $J_+ = J_-^\dagger$) implements the desired transition. The superscript k indicates the site onto which the operator acts, while γ is the rate at which the transition occurs.

The coherent dynamics, see also Fig. 1(b), is governed by the Hamiltonian

$$H = \sum_k \left[\Omega_1 \lambda_1^{(k)} + \Omega_2 \Pi_\bullet^k \lambda_6^{(k)}\right], \tag{3}$$

where we have defined the (Gell-Mann matrices) $\lambda_1 = |\bullet\rangle\langle *| + \mathrm{h.c.}$ and $\lambda_6 = |*\rangle\langle\circ| + \mathrm{h.c.}$ The operator $\Pi_\bullet^k$ implements the dynamical constraint required for the infection process [cf. Fig. 1(b)] and its precise structure depends on the lattice geometry.

The quantum master equation (1) governs the dynamics of the average (in general mixed) state. At the level of quantum trajectories [16], the quantum state is pure for all times but follows a piece-wise deterministic evolution: the state evolves according to the deterministic (non-linear) equation

$$\frac{d}{dt}|\psi_t\rangle = \left[-\mathrm{i}H_{\mathrm{eff}} + \mathrm{i}\,\langle\psi_t|\,H_{\mathrm{eff}}\,|\psi_t\rangle\right]|\psi_t\rangle\,, \tag{4}$$

where $H_{\mathrm{eff}} = H - \frac{\mathrm{i}\gamma}{2}\sum_k J_+^{(k)}J_-^{(k)}$ is the (non-Hermitean) effective Hamiltonian. However, at random times, a transition $|*\rangle \to |\circ\rangle$ occurs at a random site k, resulting in an abrupt jump of the quantum state $|\psi_t\rangle \to J_-^{(k)}|\psi_t\rangle$. This means that the k-th unit has healed (it can get infected again). More precisely, the transition rate for site k is given by $w_t^k = \gamma\langle n_*^{(k)}\rangle_t$, with $n_* = |*\rangle\langle *|$ and $\langle\cdot\rangle_t$ denoting the quantum expectation value with respect to the state $|\psi_t\rangle$. After a jump, the dynamics under Eq. (4) resumes until the next jump occurs.

The effective Hamiltonian has complex eigenvalues c_i, whose imaginary part $r_i = -\mathrm{Im}(c_i)$ is (half of) the escape rate from the associated eigenstate. The survival probability of a general state $|\psi\rangle$, i.e. its probability to evolve according to Eq. (4) for a time t without jumps, is $s_t(|\psi\rangle) = \left\|e^{-\mathrm{i}H_{\mathrm{eff}}t}\,|\psi\rangle\right\|^2$. The state with all healthy units, $|\mathrm{D}\rangle = \bigotimes_{k=1}^N |\circ\rangle^{(k)}$, cannot be left once reached dynamically. Indeed, we have $s_t(|\mathrm{D}\rangle) = 1$, meaning that the state will experience zero jumps with probability 1. Mathematically, this is a consequence of $|\mathrm{D}\rangle$ being an eigenstate of H_{eff}, associated with the eigenvalue 0. Thus, $|\mathrm{D}\rangle$ has escape rate $r_{\min} = 0$ and is invariant under the evolution in Eq. (4). It is an exact dark state for any N. In what follows, we show that, for $N \to \infty$ and for sufficiently large Ω_2, H_{eff} develops a second smallest escape rate r_{gap} (the "gap" of H_{eff}), such that $r_{\mathrm{gap}} \to 0$. This vanishing escape rate is related to an emergent (second) dark state $|\mathrm{D_e}\rangle$, which, has a finite density $\varrho_\bullet$ [see Fig. 1(c)]. This determines a phase transition between dark states in the steady state of the average quantum dynamics.

Infinite dimension.— To establish the existence of the nonequilibrium dark space phase transition, we first focus on the limit of an infinite-dimensional lattice. Here, each site has all the others as neighbors and the constraint can be written as

$$\Pi_\bullet^k = \frac{1}{N-1}\sum_{h,h\neq k}^{N} n_\bullet^{(h)} \approx \frac{1}{N}\sum_{h=1}^{N} n_\bullet^{(h)}\,, \tag{5}$$

with $n_\bullet = |\bullet\rangle\langle\bullet|$. The constraint thus requires a finite density of contagious sites. The resulting open quantum dynamics in Eq. (1) can be exactly solved in the thermodynamic limit $N \to \infty$ [19, 20]. We can thus investigate both dynamical and stationary values for the density of sites, as well as the coherence measured by the operator $\lambda_4 = |\bullet\rangle\langle\circ| + \mathrm{h.c.}$ (see Supplemental Material [21]). Throughout, we consider the state in which all units are

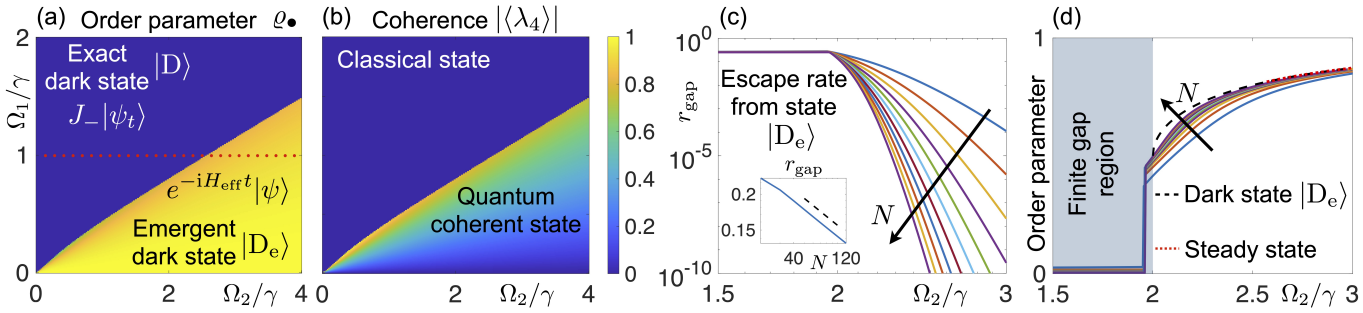

FIG. 2. **Infinite-dimensional lattice**. (a) Stationary behavior of the density of contagious sites $\varrho_\bullet$, which is an order parameter for the dark space phase transition. One phase is dominated by the classical jumps $|*\rangle \to |\circ\rangle$, bringing the system towards the state $|\mathrm{D}\rangle$. The other is dominated by the "no jump" dynamics under H_{eff}, which drives the system towards the dark state $|\mathrm{D_e}\rangle$. (b) Finite expectation values of λ_4 demonstrate that $|\mathrm{D_e}\rangle$ features coherence between states $|\bullet\rangle$ and $|\circ\rangle$. (c) Log-log plot of the gap (r_{gap}) of H_{eff} for $\Omega_1 = \gamma$ as a function of Ω_2/γ. This quantity is half the escape rate from the dark state $|\mathrm{D_e}\rangle$ and rapidly vanishes for increasing N, when $\Omega_2 > 2\Omega_1$. In the inset we show the behavior of r_{gap} as a function of N for the critical rate $\Omega_2 = 2$. The curve $N^{-0.3}$ (dashed line) is shown for comparison. (d) Average density $\varrho_\bullet$ for the eigenvector of H_{eff} associated with the gap. This shows a phase transition, from a region where the density is zero to a region where the density is finite. For increasing N, the numerical results approach the analytic prediction. Highlighted in red, the region where the average dynamics starting from $|\mathrm{U}\rangle$ approaches the dark state $|\mathrm{D_e}\rangle$. The finite N curves are for $N = 20, 30, 40, \ldots 120$.

contagious, $|\mathrm{U}\rangle = \bigotimes_{k=1}^{N} |\bullet\rangle^{(k)}$, as initial state. For weak infection rate Ω_2, the dynamics features a unique steady state — the dark state $|\mathrm{D}\rangle$. As Ω_2 increases, two further stationary states emerge which contain a finite density of contagious sites. To understand whether these are dynamically relevant we have numerically integrated the equations of motion and found that only one of them can be approached dynamically [as shown in Fig. 2(a)]. This is indeed the emergent pure dark state $|\mathrm{D_e}\rangle$.

It is interesting to investigate how the two dark states, $|\mathrm{D}\rangle$ and $|\mathrm{D_e}\rangle$, which constitute nonequilibrium phases are approached from the initial state. Approaching state $|\mathrm{D}\rangle$, the dynamics is dominated by quantum jumps, which take the system towards this classical dark state. The approach to state $|\mathrm{D_e}\rangle$ is instead dominated by the no-jump evolution under the effective Hamiltonian H_{eff}. In this regime, even if quantum jumps occur, the deterministic dynamics in Eq. (4) prevails and eventually brings the system towards the emergent dark state $|\mathrm{D_e}\rangle$, which features quantum superposition of contagious and healthy states, see Fig. 2(b). The emergence of the second dark state implies that $H_{\mathrm{eff}}|\mathrm{D_e}\rangle = c_2|\mathrm{D_e}\rangle$, with $r_2 = r_{\mathrm{gap}} = -\mathrm{Im}\, c_2 \to 0$ in the thermodynamic limit. This indeed means that the dynamics in Eq. (4) has also the state $|\mathrm{D_e}\rangle$ as a fixed point, and that $s_t(|\mathrm{D_e}\rangle) = 1$, so that this state is protected against quantum jumps.

To verify this picture, we have diagonalized H_{eff} and studied its spectrum in the sector of fully symmetric many-body states (see Ref. [21]). In Fig. 2(c), we see that there is a range of Ω_2-values where the gap, r_{gap}, remains finite. Here the system has $|\mathrm{D}\rangle$ as the sole steady state. For larger Ω_2, the gap decreases with system size with a trend that indicates a rapid convergence to zero for $N \to \infty$ [21]. At the critical point the gap decays with a power-law behavior $r_{\mathrm{gap}} \propto N^{-0.3}$, see inset in Fig. 2(c). As shown in Fig. 2(d), the first "excited" state of H_{eff} develops, in the supercritical region, a finite density of contagious sites $\varrho_\bullet$ which tends to the steady state prediction obtained for the Lindblad dynamics. This eigenvector is the emergent dark state $|\mathrm{D_e}\rangle$. As demonstrated in [21], this state does not only feature single-site coherence [cf. Fig. 2(b)] but also quantum correlations.

One-dimensional lattice.— We now focus on a $1D$ lattice, where a given site k has only two neighbors and the constraint $\Pi_\bullet^k$ reads as

$$\Pi_\bullet^k = \frac{n_\bullet^{(k-1)} + n_\bullet^{(k+1)}}{2}. \tag{6}$$

For this setting, no analytical solution is possible. We therefore rely on extensive numerical investigations to show the emergence of the dark state $|\mathrm{D_e}\rangle$ [21].

In Fig. 3(a-b) we show results obtained from sampling quantum trajectories for a few-body system up to a finite time t. The "phase diagram" displays a behavior similar to what we observed for the infinite-dimensional lattice. However, in this case, the appearance of the dark state $|\mathrm{D_e}\rangle$ is only possible for a transient period of time, given that, for finite N, the unique steady state is the exact dark state $|\mathrm{D}\rangle$. Representative trajectories for larger system sizes [see top and bottom trajectories in Fig. 1(c)] show clearly how one phase is reached when quantum jumps are dominating the dynamics, while the other one is approached when the system state is driven towards the emergent dark state by the effective Hamiltonian.

To talk about a proper nonequilibrium phase transition in the quantum system, we need to address the thermodynamic limit of an infinitely long chain. We do this by exploiting methods based on matrix product states (MPSs) [27–30]. In order to show the emergence of the

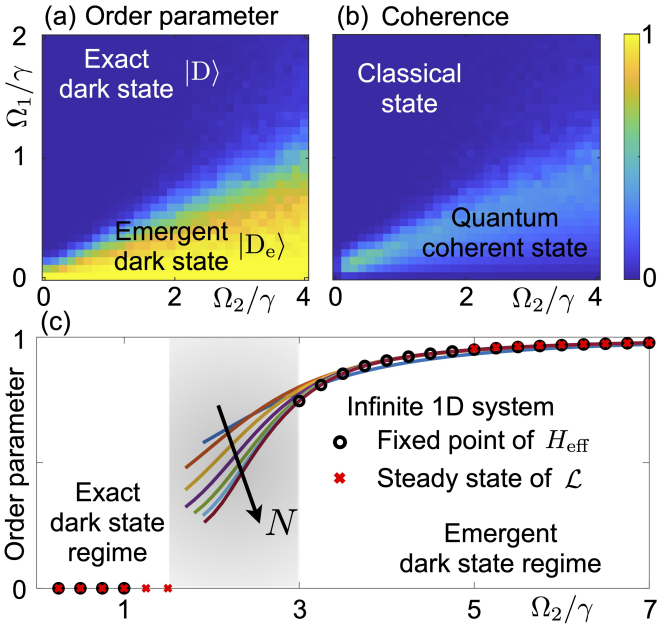

FIG. 3. **One-dimensional lattice**. (a-b) Simulations of quantum jump trajectories, for a $1D$ system with $N = 6$. Each data point is obtained by averaging over 100 trajectories. The panels show the behavior of the density of contagious sites $\varrho_\bullet$ and of the coherence $|\langle\lambda_4\rangle|$, for $t = 20/\gamma$. Two different phases emerge: one is the dark state $|D\rangle$, while, in the other the system approaches the emergent dark state $|D_e\rangle$. (c) Order parameter $\varrho_\bullet$ as a function of Ω_2, for $\Omega_1 = \gamma$ in the emergent dark state. For finite systems, this is estimated by looking at properties of the state associated with the gap of the effective Hamiltonian (solid lines for $N = 3, 4, \dots 9$). For infinite systems, we exploit matrix product state methods to target the fixed point of the dynamics in Eq.(4) (black circles). This shows a transition from $|D\rangle$ to $|D_e\rangle$. We have further obtained values of the density $\varrho_\bullet$ in the steady state of the Lindblad dynamics Eq.(1) (red crosses), which are in agreement with the prediction made for $H_{\rm eff}$. In the shaded region, our MPS algorithms did not converge.

second dark state $|D_e\rangle$ in the effective Hamiltonian, we simulate the dynamics in Eq. (4) for an infinite system, starting from the state $|U\rangle$, until a fixed point is reached. In the regime associated with the exact dark state this dynamics always ends up in the state $|D\rangle$. For sufficiently large values of Ω_2, instead, the effective time-evolution converges towards the emergent dark state $|D_e\rangle$, featuring a finite density of contagious sites $\varrho_\bullet$ and finite coherence $\langle\lambda_4\rangle$ [21]. Close to the critical regime [shaded region in Fig. 3(c)] the bond dimension χ of the MPS needed for approximating the order parameter increases, indicating that the state acquires longer-ranged correlations. For instance, for $\Omega_2/\gamma = 3$, we used $\chi = 64$ while far from the critical regime, where the emergent dark state tends to become uncorrelated, we achieved good convergence with $\chi \approx 4, 8$. Through a similar MPS algorithm, we have also studied the Lindblad dynamics (1) for an infinite system. For the model considered, this method showed instabilities for large dimensions of the MPS. We have thus exploited a low-rank approximation of ρ_t, which may be regarded as a "perturbative" approach [21] beyond a product-state ansatz which can account for very short-range correlations, and is expected to be valid for large enough Ω_2. Our results show that the emergent dark state $|D_e\rangle$ approached by the dynamics in Eq. (4), is also the steady state of the average quantum dynamics [see Fig. 3(c)].

Towards an experimental implementation.— For the purpose of this work Hamiltonian (3) should be regarded as an idealized model. However, as we briefly sketch in the following, one may indeed realize versions of it on current quantum simulator platforms based on Rydberg atoms [31–37]. Here, the three states are represented by atomic Rydberg states which interact with a nearest-neighbor density-density interaction, parametrized by the matrix $V_{\alpha\beta}$ ($\alpha, \beta = \bullet, *, \circ$). The interaction Hamiltonian of a single atom with its left (L) and right (R) neighbor is then given by

$$H_{\rm int} = \sum_{\alpha,\beta=\bullet,*,\circ}^{3} V_{\alpha\beta}(n_\beta^{(\rm L)} + n_\beta^{(\rm R)})n_\alpha.$$

The atoms are also driven by two lasers which couple the transitions $|\bullet\rangle \leftrightarrow |*\rangle$ (Rabi frequency Ω_1) and $|*\rangle \leftrightarrow |\circ\rangle$ (Rabi frequency Ω_2). By appropriately choosing the laser detunings and the coefficients of the interaction matrix $V_{\alpha\beta}$, and moving into a suitable interaction picture [21], one obtains (in $1D$) the constrained Hamiltonian [38–49]

$$H_{\rm exp} \approx \sum_k \Big[\Omega_1 \left(1 - n_\circ^{(k-1)}\right)\left(1 - n_\circ^{(k+1)}\right)\lambda_1^{(k)} + \\ + \Omega_2 \left(n_\bullet^{(k-1)} + n_\bullet^{(k+1)} - 2n_\bullet^{(k-1)}n_\bullet^{(k+1)}\right)\lambda_6^{(k)}\Big].$$

This is similar to the Hamiltonian (3), with two differences: a constraint on the transition $|\bullet\rangle \leftrightarrow |*\rangle$ and a term proportional to $n_\bullet^{(k-1)}n_\bullet^{(k+1)}\lambda_6^{(k)}$. The former is not problematic, since the transition would be anyway switched off when the dark state $|D\rangle$ is reached. The latter term, instead, changes the behaviour of the model, as we have tested with numerical simulations. However, this can be eliminated by generating the same term with opposite sign through the application of a further laser field with a detuning $2V_{\bullet\circ}$ and Rabi frequency $2\Omega_2$, on the $|*\rangle \leftrightarrow |\circ\rangle$ transition. The computation demonstrating how this can be achieved, has been presented in Refs. [13, 50].

Discussion.— We have investigated a novel type of nonequilibrium phase transition between two dark states, a trivial (classical) one and an emergent one. As we have shown, the detection of such an emergent state is possible by analyzing the spectral properties of the effective Hamiltonian. It is important to comment on why such a phenomenology cannot be observed in classical models.

Here, a non-fluctuating state can only be a configuration state, as for example $|\mathrm{D}\rangle$, and thus can only be dark if it is an exact dark state for any system size. Furthermore, in classical settings, there is no effective coherent dynamics between jumps that could drive the system toward an emergent dark state. The dark state observed here is further rather different in nature to the usual dark states that have been explored in several quantum systems [51–55], since it is not a frustration-free exact dark state for any system size (see, however, Ref. [56] for another example beyond this paradigm). Our results further show that the emergent dark state is a (pure) many-body state featuring correlations and entanglement. In one dimension and far from criticality, correlations are short-ranged (as witnessed by the low bond dimension needed for its approximation) but become increasingly longer ranged approaching the phase transition point. In infinite dimensions, correlations are of collective type with diverging susceptibility at the critical point [21].

Degenerate dark state manifolds may also emerge in finite-size dissipative noninteracting topological systems, and are usually associated with the existence of localized (edge) zero modes [57, 58]. However, we note that the mere existence of a dark subspace is not sufficient to observe the dark space phase transition discussed here. For the noninteracting physics described in Refs. [57], the dark subspace plays more the role of a decoherence-free subspace where the initial "occupation" of the zero modes is protected and fully determines whether the asymptotic state is mixed or pure. Instead, the dark state $|\mathrm{D_e}\rangle$ emerges in the thermodynamic limit as a collective property of the system. In addition, the dynamics always drives the system into one of the two possible dark states [see, e.g., our analysis for the infinite-dimensional lattice] and not into a mixture, that depends on the initial conditions. This mechanism is a necessary ingredient to observe a dark space phase transition.

We acknowledge support from the "Wissenschaftler Rückkehrprogramm GSO/CZS" of the Carl-Zeiss-Stiftung and the German Scholars Organization e.V., as well as through The Leverhulme Trust [Grant No.RPG-2018-181], the UK Engineering and Physical Sciences Research Council (EPSRC) [Grant No. EP/R04421X/1], and the Deutsche Forschungsgemeinschaft through SPP 1929 (GiRyd) [Grant No. 428276754] and [Grant No. 435696605].

* Corresponding Author: federico.carollo@uni-tuebingen.de

[1] S. Lübeck, Universal scaling behavior of non-equilibrium phase transitions, International Journal of Modern Physics B **18**, 3977 (2004).

[2] M. Henkel, H. Hinrichsen, and S. Lübeck, *Non-Equilibrium Phase Transitions* (Springer Netherlands, 2008).

[3] H. Hinrichsen, Non-equilibrium critical phenomena and phase transitions into absorbing states, Advances in Physics **49**, 815 (2000).

[4] D. Mollison, Spatial contact models for ecological and epidemic spread, Journal of the Royal Statistical Society. Series B (Methodological) **39**, 283 (1977).

[5] P. Grassberger, On the critical behavior of the general epidemic process and dynamical percolation, Mathematical Biosciences **63**, 157 (1983).

[6] M. Marcuzzi, M. Buchhold, S. Diehl, and I. Lesanovsky, Absorbing state phase transition with competing quantum and classical fluctuations, Phys. Rev. Lett. **116**, 245701 (2016).

[7] R. Gutiérrez, C. Simonelli, M. Archimi, F. Castellucci, E. Arimondo, D. Ciampini, M. Marcuzzi, I. Lesanovsky, and O. Morsch, Experimental signatures of an absorbing-state phase transition in an open driven many-body quantum system, Phys. Rev. A **96**, 041602 (2017).

[8] D. Roscher, S. Diehl, and M. Buchhold, Phenomenology of first-order dark-state phase transitions, Phys. Rev. A **98**, 062117 (2018).

[9] F. Carollo, E. Gillman, H. Weimer, and I. Lesanovsky, Critical behavior of the quantum contact process in one dimension, Phys. Rev. Lett. **123**, 100604 (2019).

[10] E. Gillman, F. Carollo, and I. Lesanovsky, Numerical simulation of critical dissipative non-equilibrium quantum systems with an absorbing state, New Journal of Physics **21**, 093064 (2019).

[11] S. Helmrich, A. Arias, G. Lochead, T. M. Wintermantel, M. Buchhold, S. Diehl, and S. Whitlock, Signatures of self-organized criticality in an ultracold atomic gas, Nature **577**, 481 (2020).

[12] M. Jo, J. Lee, K. Choi, and B. Kahng, Absorbing phase transition with a continuously varying exponent in a quantum contact process: A neural network approach, Phys. Rev. Research **3**, 013238 (2021).

[13] R. Nigmatullin, E. Wagner, and G. K. Brennen, Directed percolation in non-unitary quantum cellular automata, arXiv:2105.01394 (2021).

[14] M. Fleischhauer and M. D. Lukin, Dark-state polaritons in electromagnetically induced transparency, Phys. Rev. Lett. **84**, 5094 (2000).

[15] C. Gardiner and P. Zoller, *Quantum noise: a handbook of Markovian and non-Markovian quantum stochastic methods with applications to quantum optics* (Springer Science & Business Media, 2004).

[16] M. B. Plenio and P. L. Knight, The quantum-jump approach to dissipative dynamics in quantum optics, Rev. Mod. Phys. **70**, 101 (1998).

[17] G. Lindblad, On the generators of quantum dynamical semigroups, Communications in Mathematical Physics **48**, 119 (1976).

[18] V. Gorini, A. Kossakowski, and E. C. G. Sudarshan, Completely positive dynamical semigroups of n-level systems, Journal of Mathematical Physics **17**, 821 (1976).

[19] F. Benatti, F. Carollo, R. Floreanini, and H. Narnhofer, Quantum spin chain dissipative mean-field dynamics, J. Phys. A: Math. Theor. **51**, 325001 (2018).

[20] F. Carollo and I. Lesanovsky, Exactness of mean-field equations for open dicke models with an application to pattern retrieval dynamics, Phys. Rev. Lett. **126**, 230601 (2021).

[21] see Supplemental Material, which includes Ref. [22–26], for details.

[22] O. E. Lanford and D. Ruelle, Observables at infinity and states with short range correlations in statistical mechanics, Communications in Mathematical Physics **13**, 194 (1969).

[23] A. Kshetrimayum, H. Weimer, and R. Orús, A simple tensor network algorithm for two-dimensional steady states, Nature Communications **8**, 1291 (2017).

[24] H. Weimer, Variational principle for steady states of dissipative quantum many-body systems, Phys. Rev. Lett. **114**, 040402 (2015).

[25] F. Benatti, F. Carollo, R. Floreanini, and H. Narnhofer, Non-markovian mesoscopic dissipative dynamics of open quantum spin chains, Phys. Lett. A **380**, 381 (2016).

[26] F. Benatti, F. Carollo, R. Floreanini, and H. Narnhofer, Quantum fluctuations in mesoscopic systems, Journal of Physics A: Mathematical and Theoretical **50**, 423001 (2017).

[27] G. Vidal, Efficient classical simulation of slightly entangled quantum computations, Phys. Rev. Lett. **91**, 147902 (2003).

[28] G. Vidal, Efficient simulation of one-dimensional quantum many-body systems, Phys. Rev. Lett. **93**, 040502 (2004).

[29] G. Vidal, Classical simulation of infinite-size quantum lattice systems in one spatial dimension, Phys. Rev. Lett. **98**, 070201 (2007).

[30] S. Paeckel, T. Köhler, A. Swoboda, S. R. Manmana, U. Schollwöck, and C. Hubig, Time-evolution methods for matrix-product states, Annals of Physics **411**, 167998 (2019).

[31] I. Bloch, J. Dalibard, and S. Nascimbène, Quantum simulations with ultracold quantum gases, Nature Physics **8**, 267 (2012).

[32] H. Labuhn, D. Barredo, S. Ravets, S. de Léséleuc, T. Macrì, T. Lahaye, and A. Browaeys, Tunable two-dimensional arrays of single Rydberg atoms for realizing quantum Ising models, Nature **534**, 667 (2016).

[33] M. Endres, H. Bernien, A. Keesling, H. Levine, E. R. Anschuetz, A. Krajenbrink, C. Senko, V. Vuletic, M. Greiner, and M. D. Lukin, Atom-by-atom assembly of defect-free one-dimensional cold atom arrays, Science **354**, 1024 (2016).

[34] H. Bernien, S. Schwartz, A. Keesling, H. Levine, A. Omran, H. Pichler, S. Choi, A. S. Zibrov, M. Endres, M. Greiner, V. Vuletić, and M. D. Lukin, Probing many-body dynamics on a 51-atom quantum simulator, Nature **551**, 579 (2017).

[35] A. Keesling, A. Omran, H. Levine, H. Bernien, H. Pichler, S. Choi, R. Samajdar, S. Schwartz, P. Silvi, S. Sachdev, P. Zoller, M. Endres, M. Greiner, V. Vuletić, and M. D. Lukin, Quantum Kibble–Zurek mechanism and critical dynamics on a programmable Rydberg simulator, Nature **568**, 207 (2019).

[36] A. Browaeys and T. Lahaye, Many-body physics with individually controlled Rydberg atoms, Nature Physics **16**, 132 (2020).

[37] S. Ebadi, T. T. Wang, H. Levine, A. Keesling, G. Semeghini, A. Omran, D. Bluvstein, R. Samajdar, H. Pichler, W. W. Ho, S. Choi, S. Sachdev, M. Greiner, V. Vuletic, and M. D. Lukin, Quantum phases of matter on a 256-atom programmable quantum simulator, arXiv:2012.12281 (2020).

[38] C. Ates, T. Pohl, T. Pattard, and J. M. Rost, Antiblockade in rydberg excitation of an ultracold lattice gas, Phys. Rev. Lett. **98**, 023002 (2007).

[39] B. Sun and F. Robicheaux, Numerical study of two-body correlation in a 1D lattice with perfect blockade, New Journal of Physics **10**, 045032 (2008).

[40] T. Pohl, H. Sadeghpour, and P. Schmelcher, Cold and ultracold rydberg atoms in strong magnetic fields, Physics Reports **484**, 181 (2009).

[41] C. Ates, J. P. Garrahan, and I. Lesanovsky, Thermalization of a Strongly Interacting Closed Spin System: From Coherent Many-Body Dynamics to a Fokker-Planck Equation, Phys. Rev. Lett. **108**, 110603 (2012).

[42] Y. Y. Jau, A. M. Hankin, T. Keating, I. H. Deutsch, and G. W. Biedermann, Entangling atomic spins with a rydberg-dressed spin-flip blockade, Nature Physics **12**, 71 (2016).

[43] M. M. Valado, C. Simonelli, M. D. Hoogerland, I. Lesanovsky, J. P. Garrahan, E. Arimondo, D. Ciampini, and O. Morsch, Experimental observation of controllable kinetic constraints in a cold atomic gas, Phys. Rev. A **93**, 040701 (2016).

[44] M. Marcuzzi, J. c. v. Minář, D. Barredo, S. de Léséleuc, H. Labuhn, T. Lahaye, A. Browaeys, E. Levi, and I. Lesanovsky, Facilitation dynamics and localization phenomena in rydberg lattice gases with position disorder, Phys. Rev. Lett. **118**, 063606 (2017).

[45] C. J. Turner, A. A. Michailidis, D. A. Abanin, M. Serbyn, and Z. Papić, Weak ergodicity breaking from quantum many-body scars, Nature Physics **14**, 745 (2018).

[46] C.-J. Lin and O. I. Motrunich, Exact quantum many-body scar states in the rydberg-blockaded atom chain, Phys. Rev. Lett. **122**, 173401 (2019).

[47] M. Schecter and T. Iadecola, Weak ergodicity breaking and quantum many-body scars in spin-1 xy magnets, Phys. Rev. Lett. **123**, 147201 (2019).

[48] N. Pancotti, G. Giudice, J. I. Cirac, J. P. Garrahan, and M. C. Bañuls, Quantum east model: Localization, nonthermal eigenstates, and slow dynamics, Phys. Rev. X **10**, 021051 (2020).

[49] P. Sala, T. Rakovszky, R. Verresen, M. Knap, and F. Pollmann, Ergodicity Breaking Arising from Hilbert Space Fragmentation in Dipole-Conserving Hamiltonians, Phys. Rev. X **10**, 011047 (2020).

[50] T. M. Wintermantel, Y. Wang, G. Lochead, S. Shevate, G. K. Brennen, and S. Whitlock, Unitary and Nonunitary Quantum Cellular Automata with Rydberg Arrays, Phys. Rev. Lett. **124**, 070503 (2020).

[51] A. Griessner, A. J. Daley, S. R. Clark, D. Jaksch, and P. Zoller, Dark-state cooling of atoms by superfluid immersion, Phys. Rev. Lett. **97**, 220403 (2006).

[52] S. Diehl, A. Micheli, A. Kantian, B. Kraus, H. P. Büchler, and P. Zoller, Quantum states and phases in driven open quantum systems with cold atoms, Nature Physics **4**, 878 (2008).

[53] B. Kraus, H. P. Büchler, S. Diehl, A. Kantian, A. Micheli, and P. Zoller, Preparation of entangled states by quantum markov processes, Phys. Rev. A **78**, 042307 (2008).

[54] S. Diehl, E. Rico, M. A. Baranov, and P. Zoller, Topology by dissipation in atomic quantum wires, Nature Physics **7**, 971 (2011).

[55] B. Buča, C. Booker, M. Medenjak, and D. Jaksch, Bethe ansatz approach for dissipation: exact solutions of quantum many-body dynamics under loss, New Journal of

Physics **22**, 123040 (2020).
[56] A. Tomadin, S. Diehl, and P. Zoller, Nonequilibrium phase diagram of a driven and dissipative many-body system, Phys. Rev. A **83**, 013611 (2011).
[57] C.-E. Bardyn, M. A. Baranov, C. V. Kraus, E. Rico, A. İmamoğlu, P. Zoller, and S. Diehl, Topology by dissipation, New Journal of Physics **15**, 085001 (2013).
[58] S. Lieu, M. McGinley, and N. R. Cooper, Tenfold way for quadratic lindbladians, Phys. Rev. Lett. **124**, 040401 (2020).